NAIC-ID(RS)T-0202-95

NATIONAL AIR INTELLIGENCE CENTER

RESEARCH ON LARGE ASTRONOMICAL TELESCOPES

by

Ma Binzhong

Approved for public release: distribution unlimited

HUMAN TRANSLATION

NAIC-ID(RS)T-0202-95 7 July 1995

MICROFICHE NR: 95C0004D2

RESEARCH ON LARGE ASTRONOMICAL TELESCOPES

By: Ma Binzhong

English pages: 26

Source: Zhongguo Kongjian Kexue, Vol. 13, Nr. 5, 1993; pp. 6-14

Country of origin: China
Translated by: Leo Kanner Associates
F33657-88-D-2188
Requester: NAIC/TASC/Lt Shaun M. McMahon
Approved for public release: distribution unlimited.

GRAPHICS DISCLAIMER

All figures, graphics, tables, equations, etc. merged into this translation were extracted from the best quality copy available.

RESEARCH ON LARGE ASTRONOMICAL TELESCOPES

Ma Binzhong

Nanjing Development Center for Astronomical Instruments, Chinese Academy of Sciences

ABSTRACT

It was proposed to build a 4.3-m optical infrared new-technology telescope, which will be on-line via a vacuum piping with a 2.16-m telescope at the Beijing Astronomical Observatory for CCD photographic and light interference measurements. Thus, the light-collecting capability is upgraded to a telescope of 4.8-m aperture with resolving power of 10-m aperture.

Key words: astronomical telescope, design scheme, research.

I. Introduction

Modern astronomical and space sciences, as well as aerospace activities, urgently require research on stellar system formation, distribution, structure, and evolution in deep space, as well as their risks and influences on mankind by their violent physical processes. To explore whether there is life elsewhere

in the universe and a series of other problems of whether or not the universe can be utilized for mankind's production and livelihood services, astronomers and aerospace scientists urgently require larger-aperture astronomical telescopes to observe darker, smaller, and more remote stars and spacecraft in order to discover new heavenly bodies, as well as to track and observe spacecraft for determinations of their shape, size, coordinates, and motion. Higher resolving power can be used to study the details of the fine structure and attitude. With light measurement and spectrum analysis, the mass composition as well as physical and chemical properties can be revealed so that mankind can have further understanding of the universe. Therefore, the former Soviet Union, the United States, and China launched numerous interstellar probes, space telescopes, and various scientific experimental satellites, in addition to the development of large astronomical telescopes [3-6].

According to feasible financial and technical resources and available equipment conditions, China proposed first to build a 4.5-m optical infrared new-technology telescope, which will be on line with a vacuum piping with a 2.16-m telescope, for light interference measurements. The resolving power of the complex corresponds to a telescope with an aperture of more than 10m. The light-collecting capability of noncoherent light beams corresponds to a telescope of 4.8-m aperture, as shown in Fig. 1. This scheme is low in construction costs, short in provisional fabrication period, and can meet the requirements of multiple

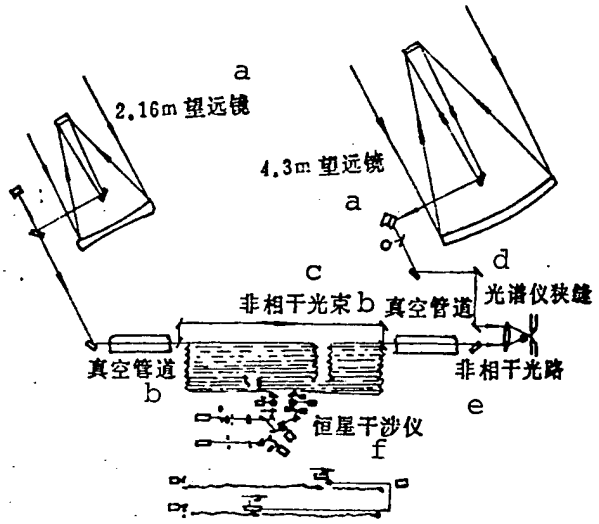

Fig. 1. Principles of fixed-star light interference system, and light collecting system of noncoherent light
KEY: a - telescope b - vacuum piping c - noncoherent light beam d - narrow gap of spectrum instrument e - noncoherent light path f - fixed-star interferometer

applications. This is a relatively rational scheme meeting China's situation. This comprehensive aperture scheme [10, 12] can utilize the available site and 2.16-m telescope of the Beijing Observatory. This scheme has better practical feasibility compared to fabricating several new telescopes and new sites to be built.

II. Selection of Models

At present, there are the following models of telescopes developed abroad.

(1) Single-Lens Surface Telescope [5]

An entire block of primary lens structure of an 8-m

telescope is adopted with features of high light-collecting capability and high resolving power, suitable for infrared observation, as well as reliable and simple techniques. Therefore, China's 4.3-m telescope also adopts single-lens surface. However, the single-lens surface is restricted by blank fabrication and machining, as well as framework structure. Therefore, at present the largest single-lens surface telescope in the plan has an 8m aperture.

(2) Compound Telescope [3]

For instance, for a 10-m telescope at Keck in the United States, 36 blocks of hexagonal lenses with 1.8m side-to-side are assembled into a 10-m telescope. The advantages are light in weight and relief from difficult machining of large 10-m lens surfaces, thus reducing fabrication costs. However, it is difficult to machine the hexagonal off-axis paraboloid-surface lens with complex control systems. Its light-collecting capability and resolving power are inferior to those of single-lens-surface telescopes. Especially, the 3-mm side gaps of hexagonal lenses are sources of infrared radiation, thus affecting infrared observations, as its shortcoming. Therefore, this scheme is not considered for China's 4.3-m telescope, for the time being.

(3) Assembled Telescopes

In the case of the NNTT 15-m telescope and the MMT 4.5-m

telescope in the United States, several independent primary telescope systems are assembled into a framework with a pitch and directional transmission control system, as well as a guiding star and tracking system. In this scheme, it is more difficult to operate in the infrared zone in addition to more difficult fabrication of such giant telescope frame. Therefore, this scheme is not suitable in fabricating super-large telescopes.

(4) Combinational Telescopes [6]

For instance, the VLT of the European Community, four independent 8-m telescopes are combined into a 16-m aperture; its resolving power can be further upgraded with light interference. Since the system is composed of independent telescopes, limitations from machining and structure are absent. Therefore, this scheme will be the developmental direction for super-large telescopes in the future.

III. Design of 4.3-m Optical Infrared New-Technology Telescope

At present, single-lens telescopes with aperture greater than 3.5m have been fabricated in several countries. Consideration is given to conditions of light, machining, electrical processing and assembly, in addition to site; China selects the 4.3-m aperture telescope.

3.1. Selection of Installation

At present, most intermediate and small telescopes in the

world are equatorial types, with the advantages of no visual field rotation, no zenith blind zone, minimum atmospheric refraction, good vision stability, and not requiring coordinate conversion. There are the following installation types: symmetric fork type, equatorial yoke type, polar axis type, floating ball type, and horseshoe type. Most large telescopes abroad apply horizontal type [1, 2] because of its small size, symmetric structure, good force-acting conditions, low price, and easy tracking observation of fixed stars, planets, satellites, and spacecraft. At the Nasmyth focus, various large and heavy instruments for light measurement, spectrum, and photography can be installed. There are the three following shortcomings.

1. A computer is required for coordinate transformations; however, the real-time revision is easy if a microcomputer is used. For example, it is known that the latitude of the observational station is phi, the declination is delta, and the right ascension hour angle is t, for the star to be measured, the higher and the lower angles are z and the positional angle is A for the telescope computed based on astronomical spherical triangles.

Since

$$\left.\begin{aligned} \cos z &= \sin\varphi\sin\delta + \cos\varphi\cos\delta\cos t \\ \sin z\sin A &= \cos\delta\sin t \\ \sin z\cos A &= \cos\delta\sin\varphi\cos t - \sin\delta\cos\varphi \end{aligned}\right\} \qquad (1)$$

by deduction, we obtain

$$A = \operatorname{arctg}\frac{\cos\delta\cdot\sin t}{\cos\delta\sin\varphi\cos t - \sin\delta\cos\varphi}$$

$$Z = \operatorname{arctg}\frac{\cos\delta\cdot\sin t}{\sin A(\sin\varphi\sin\delta + \cos\varphi\cos\delta\cos t)} \qquad (2)$$

2. It is required to use a Dove lens by rotating one-half parallax angle to cancel the rotation of the image field. In order to be able to apply the 3.0 to 15micrometer waveband, three blocks of plane lens are used to substitute for the Dove lens, while also applying the differential mechanism of bevel gears.

3. There is a 0.2° blind spot in the zenith region.

3.2. Optical System and Probe

In Fig. 2, if the R-C cassegrain system has a primary focus ratio f/2 for high light-collecting power, the primary lens is a concave doubled-curved surface, and the secondary lens is a convex double-curved surface, the spherical aberration and the coma aberration of all high-power light rays can be eliminated. Three revision lenses are used to upgrade the image quality with the 1° field of view. The 10-cm thin crescent primary lens is controlled by 68 active optical executing devices, and a Shack-Hartman wavefront probe (68microlenses and a CCD surface array), so that the precision of the surface shape is controlled within lambda/20. To ensure a strict alignment relationship between the microlens array and the probe, reference plane waves are introduced in the optical path. Only by precisely measuring the focal distance between the measured wave and the reference wave in each sampling element, the average inclination amount of the corresponding wave surface can be obtained. For example, the

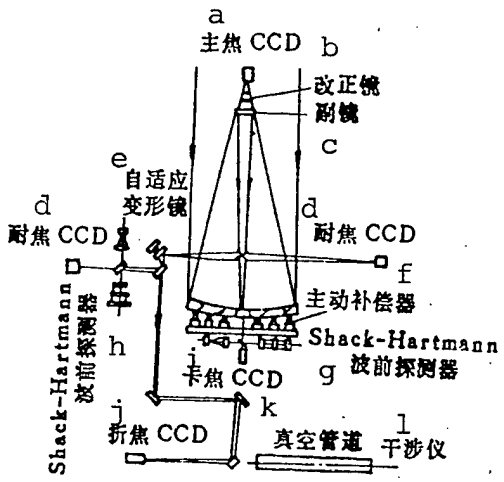

Fig. 2. Optical system of 4.3-m optical infrared new-technology telescope
KEY: a - principal focus b - correction lens
c - secondary lens d - CCD focus resistance
e - self-adaptive transformation lens
f - primary compensator g - wavefront detector
h - wavefront detector i - CCD card focus
j - CCD refraction focus k - vacuum piping
l - interferometer

inclination amounts of the wave surface in the i-th sampling element relative to the x- and y-directions are:

$$Q_{xi} = \frac{\bar{x}_i - x_i}{f} \qquad Q_{yi} = \frac{\bar{y}_i - y_i}{f} \tag{3}$$

In the equations, x_i, y_i indicate the positions of the optical axis of the i-th microlens; and $\bar{x}_i$ and $\bar{y}_i$ indicate the positions of the center of moment of the light spot in the x- and y-directions.

The structure in this scheme is simpler than that of the shear interference method. By just using one CCD surface array and a microlens surface array, random phase wavefront parameters can be determined (in other words, when the phase difference in

the element is greater than 2pi, the wave surface inclination can also be determined). The light utilization rate is 100%, thus suitable for white light as a low-cost and reliable scheme. If an artificial light source is applied, the observed stellar magnitude is not lowered because artificial light is applied on the detection wave surface. In this way, the primary focus can be used to detect very remote dark heavenly bodies. Matching with a highly sensitive large field-of-view camera, such as the 2048x2048 surface array CCD camera with high quantum efficiency, the partial visual frequency signals can be used for highly sensitive CCD guiding star.

In order to expand the observed wave sector to 15micrometers in detecting, sky gazing, and infrared star charts of infrared targets, as well as the measurement of dark light sources for spectrum analysis and increasing the instrument utilization rate in infrared observations during daytime and nights with a bright moon, we can use a card focus system, with f/15 as the focal ratio, 10 to 20Hz variable frequency, and 4' swinging amplitude for the secondary lens, along with focus adjustment. In addition, the CCD camera and guiding installation are installed on the card focus with TV monitoring, photon counter, infrared light and spectrum instrument. At the first resistance focus, a 95-element self-adaptive compensation deformation lens [9] and a Shack-Hartman wavefront detector (97 microlenses and a CCD surface array) are used so that image quality can be improved with wavefront error compensation at the infrared zone between

1.5 and 15micrometers, thus, the star spot diffused image disk is smaller than 1". For a focal ratio f/13, with a CCD camera and a guiding installation installed on the focal surface with a highly sensitive camera and TV monitoring, observation of precise structure image diagram can be observed with high resolving power approaching the limit of visual steadiness. At the second resistance focus, there are installed with the CCD camera and guiding apparatus with TV monitoring, photon counter, polarimeter, multitarget multioptical fiber spectrograph [8], and high-resolution spectrum instrument, high resolving power images can be obtained with multitarget spectrum, intermediate dispersion stellar spectrum, brightness, and polarized observations. There are units for quickly, precisely, and conveniently changing instruments. The focal ratio is f/35 for the refraction focus system; the CCD camera and guiding apparatus are installed at the focus surface in addition to a grating spectrograph and Fabry-Perot interferometer for observation of brighter fixed stars with high resolving power graph, for measurements of high dispersion and high resolution spectra and brightness. Through the vacuum piping, the image quality is good without anomalous star images as the star images through the 2.16-m lens overlapped on the CCD optical sensor surface. By using a multiple imaging computer for overlapping images, a further increase in photographic brightness results in a higher resolving power of star observations. By transmitting the star image to the optical interference system, this resolving power

equivalent to a more than 10-m aperture can be obtained. The secondary lens and the focal plane parameters are shown in Table 1. The coordinate method [11] is used to inspect the machining of the primary and secondary lenses, thus reducing the effect on inspection precision from the atmospheric turbulence. In addition, inspection with high-order aspherical surface lenses is convenient. At the lateral surface of the intermediate block, a 15-cm star guiding lens is installed for sky gazing for a large visual field with focal ratio f/5, visual field 4°, magnifying power 40, adjustable visibility, with TV monitoring and remote control.

3.3. Mechanical System

Fig. 3 shows the horizontal type structure of a 4.3-m optical infrared new-technology telescope. To ensure light alignment and stable support, a framework is welded with a fast heat-equilibrium, lightweight, and open type triangular Serrueier seamless steel pipe. When the telescope barrier points to a random position, it is required that the relative bending of the primary and secondary lens be smaller than 0.03mm, and that the relative dip angle be smaller than 2". For rigidity and compact structure for lower fabrication costs, the framework integrated change structure on the secondary lens chamber, it is not used, but the fixation of the secondary lens chamber and framework, as shown in Fig. 4, is used. However, the secondary lens casing can be turned by 180° in order to change the structure of the

TABLE 1. Parameters of Secondary Lens and Focal Surface

焦[a]点	焦[f]比	焦距/m[g]	主副镜间距/m[h]	副镜直径/m[i]	主镜凹面到焦面间距/m[j]
主焦[b]	f/2	8.6	—	—	—
耐焦[c]	f/13	55.9	7.21	0.76	3.8+2
卡焦[d]	f/15	64.5	7.41	0.65	1.5
折焦[e]	f/35	150.5	7.24	0.75	18.5+2

KEY: a - focus b - primary focus c - resistance focus d - card focus e - refraction focus f - focal ratio g - focal length h - gap between principal and secondary lenses i - diameter of secondary lens j - gap from primary-lens concave surface to focal surface

refractive focus and resistance focus secondary lenses, as shown in Fig. 5. Since there are requirements of swinging amplitude, swinging frequency of the infrared secondary lens, only one secondary lens housing is installed. During photography of the principal focus, the secondary lens housing can be lifted out. There are structures for changing filters with focus adjustment; close-cycle control is conducted on the grating rule feedback position signals of the focus adjustment amount. The secondary lens chamber is supported with a high rigidity thin rib deviated four wing beam; the secondary lens is supported at the sides with an air cushion, fixed at the back with a vacuum suction disk. There is a light shading cylinder welded with a thin aluminum plate for the secondary lens, with convenient and reliable assembly and disassembly. As shown in Fig. 6, the intermediate block is a high-rigidity box-type multi-rib light structure,

welded with 4-cm steel plate and 1-cm thick rib plate. The external side is 5m wide and 1.4m high, and the inner light-passage space is 4.4m with an octagonal shape. There is a primary lens cover with eight divisions, controlled by four steppiung motors. At the center, there is a reflective lens mechanism of two resistance focus and refractive focus light passages for rapid change. During card focus photography, the reflective lens is parallel to the primary optical axis and away from the axis. The central light-shading cylinder and the reflective lens are spotted with an offset four-wing beam. In Fig. 7, the light thin wall multi-rib primary lens chamber is welded with a 10-mm thick steel plate into a box-shaped structure, 5m in external diameter, 0.8m in internal diameter, and 0.85m high. The primary lens (10cm thick and 3.7tons in weight) is controlled by 68 active optical compensators so that the surface shape is less than lambda/20. On phi3.9-m rings, and phi2.1-m rings, 26 and 14 axial compensators are installed. These compensators can be pushed or drawn, with a balance weight in the lateral direction. A stepping motor is used to drive the screw tap for axidirectional face shaped precision compensation. On the rings of phi3-m and phi1.2-m, 20 and 8 axidirectional thrust spring compensators are installed to constitute a stepping motor compensator. At the back of the thin primary lens, 68 indium steel blocks are linked with the compensator, thus not weakening the rigidity and strength of the primary lens. There is a positioning socket in the inner hole of the primary lens to

ensure that the center of the primary lens is at the primary optical shaft, which is not under a load bearing. At the upper end of the primary lens there is a safety limiting position plate. The bottom and lateral surface are coated with an insulated layer so that the heat resistance is homogeneous at the back of the primary lens. Beneath the primary lens chamber there is a wave surface detector and various kinds of card focus observation instruments.

As shown in Fig. 3, 6-cm thick steel plates are used to weld a high-rigidity seat frame. With horizontal shafts, more than 40tons of lens barrier weight is supported. The phi600mm shaft neck is supported in the diametral and axial directions by diagonal contact bearings of 461/600. The structure is compact; the cleanliness is better than hydraulic support, without overloose matching with gaps. The high-rigidity base seat supports a load of more than 120tons. The 8687/2050 thrust ball bearing supports 80tons, while the balance is supported by 12 phi200-mmx120mm friction wheel for elastic support and transmission. The diametral-direction is positioned by two 9/1160H single-row centripetal ball bearings lubricated with force-circulation. There are crude and fine leveling mechanisms. To ensure that the telescope barrier can precisely and quickly align to any star in the celestial hemisphere with precise tracking, this requires fast guiding, slow and micro alignment for elastic support and transmission. For the DC torque motor-speed measurement set drive system with constant tracking of wide

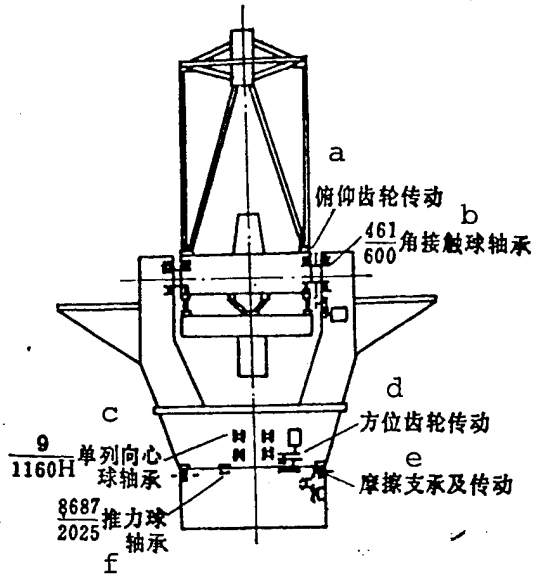

Fig. 3. Structure of 4.3-m optical infrared new technology telescope
KEY: a - dip or elevation gear transmission b - angular-contact ball bearing c - single-row centripetal ball bearing d - directional gear transmissino e - frictional support and transmission f - thrust ball bearing

range of speed adjustment, it is required that the lens barrier can pitch up and down by 0 to 95° with orientation rotating plus or minus 270°, rotating and tracking speed between 0 and 2(°)/s, and acceleration between 0 and 0.5(°)/s^2. A resolving power of 0.5" of photography lasting several hours requires stable tracking and short-cycle error less than 0.2". A 26-bit grating encoder can ensure a tracking precision of 0.2"/10min and an orientation precision of plus or minus 1.5". It is required that the rigidity of the driving system should be large, and the 8Hz mechanical resonant frequency should be avoided. Therefore, pitch transmission can apply level 5 precise straight tools cylindrical gears with number of modules m=5, number of teeth

z_1=480, and z_2=24 attached to a speed reduction gearbox with m=3 and i=20/40. For orientation transmission, level 5 precision straight teeth cylindrical gear is used, with m=6, z_I=460, and z_2=20, attacked to a speed reduction gear with m=3 and i=(20/40)x(20/80). To eliminate a tooth gap, a reverse torque motor (capable of high speed forward direction fast push) and a highly stable DC power supply are used for driving the torque motor.

3.4. Control System

To ensure that two telescopes can simultaneously track a star for observation with precision at 2" for several hours, to constitute a comprehensive aperture telescope, it is required that the precision of automatic guiding is smaller than 0.1". In addition to guiding, orientation, tracking, wavefront error detection and correction for the real-time control system, it is required to use a computer to convert between the star equatorial coordinates and the telescope horizontal coordinates. Before making observations, it is only required to input the right ascension and declination values of the star for observation, the telescope can be controlled on the maneuvering platform. In addition, computations and revisions can be made on bending and torsion of telescope barrier, shaft system deformation, transmission error, temperature compensation, refractive difference in the atmospheric, annual aberration, and planetary aberration. Ten computations per second can exhibit the

telescope working status, resolving power orientation at 1", and pitch 1". Thus, time and astronomical environmental conditions can be precisely recorded so that the error of the dome tracking telescope is plus or minus 1.5°, with safety position limitation, overload interlinking and alarming.

There are telescopes of complete automation, semi-automation, and manual control. Multiple microprocessors are used for the parallel control system, since there is high function, reliability, small size, small hardware, low cost, scattered software, and sufficient timing in execution. Operation will not be suspended entirely because of the malfunctioning of one computer. Therefore, operation and maintenance are convenient. There are the several microcomputer and single-chip processor combination systems for the control system, as follows. 1) Operation, monitoring, control, and display system; 2) orientation and tracking control, as well as status monitoring system; 3) CCD graph collection, processing and recording systems; 4) active optical and automatic optical systems for measurement and control; 5) encoding and remote control observation systems for synchronous satellites; and 6) light interference system for measurement and control

4. Design of Light Interference System of Fixed Stars

To upgrade resolving power, the vacuum piping as shown in Fig. 1 makes convergence and phase interference of focus images with refractive shaft of the 4.3-m and 2.16-m telescopes so that

the overall resolving power is higher than the milliangular second level.

4.1. Design of Conventional Light Interferometer of Fixed Stars

In order to build an instrument room with good foundation, vibration prevention, and constant temperature, it is required that the instruments are small, and are positioned between the 4.3-m and the 2.16-m telescopes. As shown in Fig. 4, in the stellar interferometer [7], it is assumed that the baseline difference b=50m of the two telescopes. When the observation celestial zone is 100° conical angle, the compensation lens of the difference of the light path is:

$$L = \frac{50 \times \cos 40^{\circ}}{16} = 2.4(\mathrm{m})$$

Sixteen reflections are made by using a reflective angular lens, the compensation length of the light-path difference is reduced. Thus, the instrument size can be small with low cost, along with reduction of effects from miscellaneous lights and atmospheric turbulence to the interference system. A 2.5-m long ballbearing tap (phi63mm) is used for transmission. A stepping motor with 0.5° steps is used in fast searching of stars. The screw tap with pitch S=10mm is used to draw the angular lens frame for star searching transmission with V_1=50mm/s; when tracking fixed stars, V_2=125micrometers/s. The lambda/10 light-path difference microadjusting compensation is made by a piezoelectric ceramic drive light wedge; the resolving power is 0.0018micrometer. The light-path difference applies the CCD inspection fringe phase and

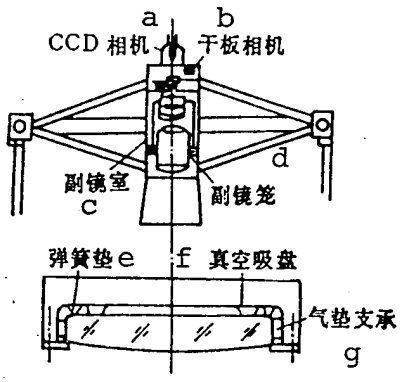

Fig. 4. Upper portion of framework, secondary lens chamber and support
KEY: a - CCD camera b - dry-plate camera c - secondary lens chamber d - secondary lens housing e - spring-mounted cushion f - vacuum suction disk g - air cushion support

contrast, looking on the white light fringe. During operation, based on the positions and variations of fixed stars during the observation time, one computes the light-path difference and its variation rate from the light to the two telescopes. Then the fast-moving and tracking angular lens frame can be controlled. Control the moving distance and velocity of the piezoceramic drive light wedge, and the CCD closed-cycle is used for monitoring and being locked on the white light fringe.

4.2. Design of Light-path Compensation Measurement System

For compact structure and reduced cost, a dual-frequency laser interferometer is used to measure the light-path difference [13] with fast star searching compensation and slow tracking compensation.

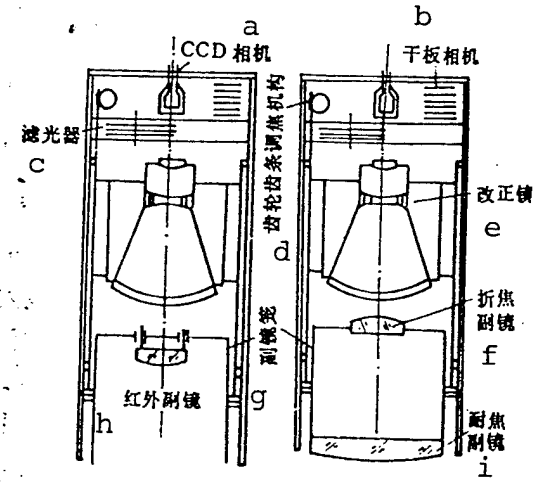

Fig. 5. Brief structural diagram of secondary lens chamber and secondary lens housing
KEY: a - CCD camera b - dry-plate camera c - filter d - rack-and-pinion focus adjustment e - correction lens f - secondary lens of refraction focus g - resistance focus h - infrared secondary lens i - secondary lens of resistance focus

1) Two Signal Channels Measured

1. The optical path measurement signals of arm A (fast speed) of the optical delay line are given by the following:

$$A_1: 2a\sin 2\pi(f_1 - f_2 \pm \Delta f_A)t \qquad A_2: 2a\cos 2\pi(f_1 - f_2 \pm \Delta f_A)t$$

2. The optical-path measurement signals of arm B (slow speed) of the optical delay line are given by the following:

$$B_1: 2a\sin 2\pi(f_1 - f_2 \pm \Delta f_B)t \qquad B_2: 2a\cos 2\pi(f_1 - f_2 \pm \Delta f_B)t$$

2) The two reference signal channels are:

$$D_1: 2a\sin 2\pi(f_1 - f_2)t \qquad D_2: 2a\cos 2\pi(f_1 - f_2)t$$

By deducting the two channel reference signals and the reference signals, we obtain:

Arm A $N_A = \int_0^t \Delta f_A dt$ Arm B $N_B = \int_0^t \Delta f_B dt$

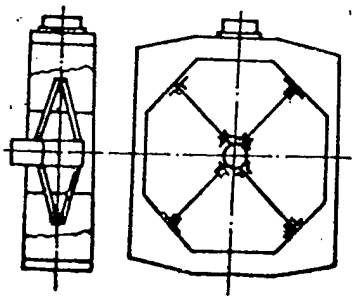

Fig. 6. Brief structural diagram of intermediate block in telescope barrel

The corresponding displacements are:

$$L_A = N_A \times \frac{\lambda}{2} \qquad L_B = N_B \times \frac{\lambda}{2}$$

To ensure measurement precision and to satisfy the requirements of light-path difference compensation lambda/10, the laser measurement system should select such products with high precision, long measurement range, high resolving power, small size, and low cost. During design, the Abbe error should be deducted so that the direction of guiding rail of the delay line is consistent with the direction (parallel or even coincident) between the motion direction and the light ray measurement direction of the measurement lens. Errors should be reduced as generated by the air path. It is required to make precise computations for stars in the celestial zone under observation, so that the initial positions of the light path-difference compensation are consistent. When the 4.3-m telescope and the 2.16-m telescope are simultaneously tracking and observing a single star, the light-path difference $\Delta = b \times \cos\theta$, as the baseline distance b between two telescopes should be compensated. This

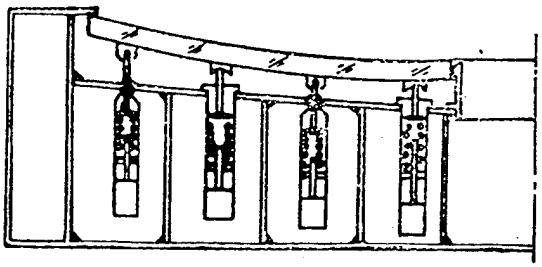

Fig. 7. Brief structural diagram of 4.3-m, crescent-shaped thin primary lens and active optical compensator

delta value has considerable difference due to differential astronomical coordinates for measurements, even this delta can be as large as the baseline length. Compensation should be made for the earth's rotation and revolution with respect to the variation of two beams of optical path difference between fixed stars. The variation of the baseline difference should be compensated due to the crustal variation, unsteady machines and thermal deformation. The variation in light-path difference due to atmospheric turbulence should be compensated for.

4.3. Parallel Compensation Measurement and Control System of Optical Axis

To improve the contrast of light interference fringes, it is required that the nonparallelness of two beams of the coherent optical wavefront should be less than 0.2". Therefore, it is required that the two telescopes synchronously track the star under observation, with the optoelectronic guidance precision better than 0.1" and tracking precision of 0.2"/min. After the deviation of a star is measured with the CCD, the piezoceramic is used to control the pitch angle of the right angle lens (range of

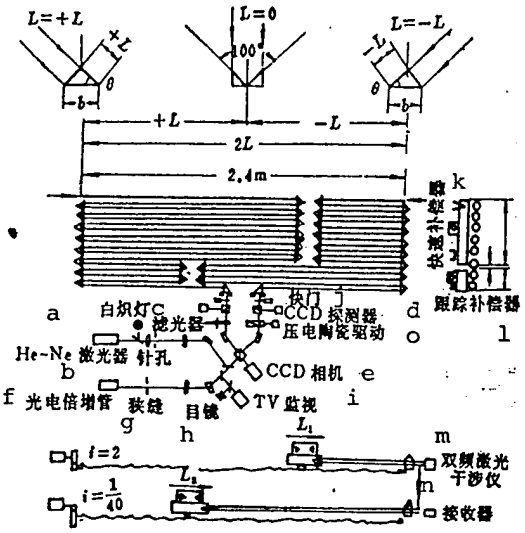

Fig. 8. Scheme of fixed-star light interferometer
KEY: a - filament lamp b - laser
c - filter d - CCD detector e - CCD camera
f - optoelectronic doubling tube g - narrow seam h - eyepiece i - TV monitoring
j - shuttle k - fast compensator l - tracking compensator m - dual-frequency laser interferometer n - receiver o - piezoelectric ceramic drive

plus or minus 30", resolving power 0.02", and frequency response 500Hz), so that the interference fringes after the coherence of the two light beams is received by the CCD.

4.4. Fringe Measurement, Analysis and Tracking of Fixed Stars

When f=500Hz, triangular waves are used to modulate a light-circuit difference compensation path for a rectangular lens. The modulation amplitude is one wavelength. If the fringe output intensity is in the singly-scanned period of PZT, the number of photons is A, B, C, and D received in four time segments. Then we obtain:

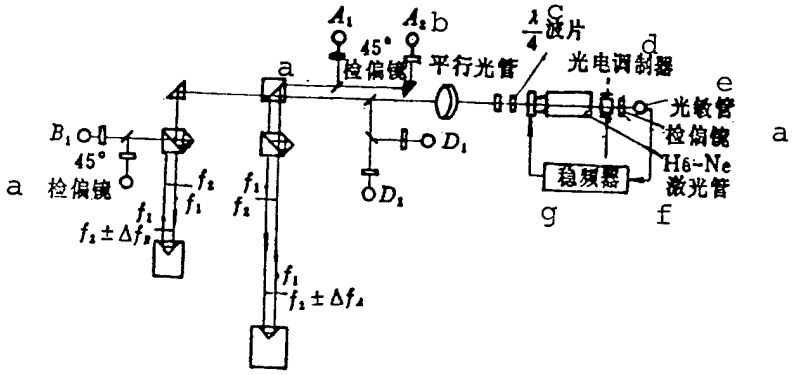

Fig. 9. Optical path diagram of light path difference compensating measurement system
KEY: a - deviation detecting lens b - parallel light tube c - quarter wavelength lens d - optoelectronic modulator e - photo-sensitive tube f - He-Ne laser g - frequency stabilizer

fringe oscillation amplitude $A_{mp} = \sqrt{(C-A)^2 + (D-B)^2}$

fringe phase $\phi = \text{arctg}\left(\frac{D-B}{C-A}\right) - \frac{\pi}{4}$

fringe contrast $V^2 = \frac{\pi^2}{12} \times \frac{(A-C)^2 + (B-D)^2 - N}{(N - D_{ark})^2}$

In the equations, N=A+B+C+D; D_{ark} is dark current.

In order to let the light-path difference be zero, it is required to have symmetrical interference fringes and a large difference between peak and valley. According to the light intensity signals received by the interference fringe in CCD imaging, the main fringes and the side lobe fringes can be determined. The light-path difference computed is:

$$D = \left(\sum_{r=1}^{R} I_r - \sum_{l=1}^{L} I_l\right) \Big/ \left(\sum_{r=1}^{R} I_r + \sum_{l=1}^{L} I_l\right)$$

In the equation, I_r is the light intensity signal of R outputs of the CCD covered by the right side lobe fringe.

I_1 is the light intensity signals outputted by L image elements of the CCD covered by the side lobe fringes.

The central fringes can be found through the CCD with tracking. The amplitude and phase of the interference fringes include the distribution information of light intensity on the surface of the heavenly body. Thus, the heavenly body parameters, such as position, angular diameter, and distance between two stars, can be measured for the fixed star.

4.5. Assembly Adjustment and Testing of Light Interferometer of Fixed Stars

For convenience in adjustment, a pseudostar system is placed on the optical circuit; the He-Ne high-interference laser is used as the self-aligned light source. After the optical circuit is completely adjusted, a filament lamp is used for adjustment until the white light interference fringes appear. After the system is completely adjusted, the spectroscope of the pseudostar system is removed so that the signal intensity of the interference fringes of the primary optical circuit is not affected.

5. Design of Circular Cylinder, Square-topped Observation Chamber for 4.3-m Telescope

To well protect the telescope and to ensure observations under optimal conditions, along with consideration of contracting

the size of the observation chamber and to reduce the cost, a cylindrical square-topped observation chamber was designed. Astronomers can make remote controlled observations on a large screen display in the control building so that the telescope is not influenced by human heat radiation and oscillation. The overall height of the square top is 35m; the height of the cement chamber is 18m; the bottom diameter of the rotating portion is 21m; and the width of the rotating space of the telescope barrier is 8.6m, and 17.5m long. At the top, there is a 15-ton hoist and a 46-ton hoisting hook. The minimum gap between the telescope and the square top is 10cm. In the square top, there are loading and unloading equipment of the primary telescope, along with lens surface cleaning, vacuum film-coating machine, as well as circulating water and air ventilation system. In the control building, there is a large television screen and remote controlled equipment, in addition to a developing room for dry photographic plates, a chamber for star charts and star tables, a computer room, a timing room, research and information chamber, and laboratories for optics, machinery, and electricity.

This paper is based on an astronomical foundation topic, Research on Models of Large Telescopes. The paper was received for publication on December 18, 1992.

DISTRIBUTION LIST

DISTRIBUTION DIRECT TO RECIPIENT

ORGANIZATION	MICROFICHE
B085 DIA/RTS-2FI	1
C509 BALLOC509 BALLISTIC RES LAB	1
C510 R&T LABS/AVEADCOM	1
C513 ARRADCOM	1
C535 AVRADCOM/TSARCOM	1
C539 TRASANA	1
Q592 FSTC	4
Q619 MSIC REDSTONE	1
Q008 NTIC	1
Q043 AFMIC-IS	1
E404 AEDC/DOF	1
E410 AFDTC/IN	1
E429 SD/IND	1
P005 DOE/ISA/DDI	1
1051 AFIT/LDE	1
P090 NSA/CDB	1

Microfiche Nbr: FTD95C000402
NAIC-ID(RS)T-0202-95